World Journal of Gastroenterology

Submit a Manuscript: https://www.f6publishing.com

World J Gastroenterol 2022 July 14; 28(26): 3132-3149

DOI: 10.3748/wjg.v28.i26.3132

ISSN 1007-9327 (print) ISSN 2219-2840 (online)

ORIGINAL ARTICLE

Basic Study

Neutrophil extracellular traps participate in the development of cancer-associated thrombosis in patients with gastric cancer

Jia-Cheng Li, Xiao-Ming Zou, Shi-Feng Yang, Jia-Qi Jin, Lei Zhu, Chang-Jian Li, Hao Yang, An-Ge Zhang, Tian-Qi Zhao, Chong-Yan Chen

Specialty type: Gastroenterology and hepatology

Provenance and peer review: Unsolicited article; Externally peer reviewed.

Peer-review model: Single blind

Peer-review report's scientific quality classification
Grade A (Excellent): 0
Grade B (Very good): B, B, B
Grade C (Good): C
Grade D (Fair): 0
Grade E (Poor): 0

P-Reviewer: Ferreira GSA, Brazil; Mohamed SY, Egypt; Morozov S, Russia; Singh I, United States

Received: October 19, 2021
Peer-review started: October 19, 2021
First decision: January 11, 2022
Revised: January 20, 2022
Accepted: March 16, 2022
Article in press: March 16, 2022
Published online: July 14, 2022

Jia-Cheng Li, Xiao-Ming Zou, Shi-Feng Yang, Lei Zhu, Chang-Jian Li, Hao Yang, An-Ge Zhang, Tian-Qi Zhao, Chong-Yan Chen, Department of Gastrointestinal Surgery, The Second Affiliated Hospital of Harbin Medical University, Harbin 150001, Heilongjiang Province, China

Jia-Cheng Li, Shi-Feng Yang, Jia-Qi Jin, Lei Zhu, Hao Yang, An-Ge Zhang, The Key Laboratory of Myocardial Ischemia, Harbin Medical University, Harbin 150001, Heilongjiang Province, China

Jia-Qi Jin, Department of Neurosurgery, The Second Affiliated Hospital of Harbin Medical University, Harbin 150001, Heilongjiang Province, China

Corresponding author: Xiao-Ming Zou, MD, PhD, Chief Doctor, Professor, Surgeon, Department of Gastrointestinal Surgery, The Second Affiliated Hospital of Harbin Medical University, No. 246 Xuefu Road, Nangang District, Harbin 150001, Heilongjiang Province, China. zou4930@163.com

Abstract

BACKGROUND

The development of venous thromboembolism (VTE) is associated with high mortality among gastric cancer (GC) patients. Neutrophil extracellular traps (NETs) have been reported to correlate with the prothrombotic state in some diseases, but are rarely reported in GC patients.

AIM

To investigate the effect of NETs on the development of cancer-associated thrombosis in GC patients.

METHODS

The levels of NETs in blood and tissue samples of patients were analyzed by ELISA, flow cytometry, and immunofluorescence staining. NET generation and hypercoagulation of platelets and endothelial cells (ECs) *in vitro* were observed by immunofluorescence staining. NET procoagulant activity (PCA) was determined by fibrin formation and thrombin–antithrombin complex (TAT) assays. Thrombosis *in vivo* was measured in a murine model induced by flow stenosis in the inferior vena cava (IVC).

RESULTS

NETs were likely to form in blood and tissue samples of GC patients compared with healthy individuals. *In vitro* studies showed that GC cells and their conditioned medium, but not gastric mucosal epithelial cells, stimulated NET release from neutrophils. In addition, NETs induced a hypercoagulable state of platelets by upregulating the expression of phosphatidylserine and P-selectin on the cells. Furthermore, NETs stimulated the adhesion of normal platelets on glass surfaces. Similarly, NETs triggered the conversion of ECs to hypercoagulable phenotypes by downregulating the expression of their intercellular tight junctions but upregulating that of tissue factor. Treatment of normal platelets or ECs with NETs augmented the level of plasma fibrin formation and the TAT complex. In the models of IVC stenosis, tumor-bearing mice showed a stronger ability to form thrombi, and NETs abundantly accumulated in the thrombi of tumor-bearing mice compared with control mice. Notably, the combination of deoxyribonuclease I, activated protein C, and sivelestat markedly abolished the PCA of NETs.

CONCLUSION

GC-induced NETs strongly increased the risk of VTE development both *in vitro* and *in vivo*. NETs are potential therapeutic targets in the prevention and treatment of VTE in GC patients.

Key Words: Neutrophil extracellular traps; Gastric cancer; Platelet; Endothelial cells; Venous thromboembolism

Core tip: We found that gastric cancer (GC)-induced neutrophil extracellular traps (NETs) strongly increase the risk of venous thromboembolism (VTE) development in GC patients. NETs are potential therapeutic targets in the prevention and treatment of VTE in GC patients.

Citation: Li JC, Zou XM, Yang SF, Jin JQ, Zhu L, Li CJ, Yang H, Zhang AG, Zhao TQ, Chen CY. Neutrophil extracellular traps participate in the development of cancer-associated thrombosis in patients with gastric cancer. *World J Gastroenterol* 2022; 28(26): 3132-3149

URL: https://www.wjgnet.com/1007-9327/full/v28/i26/3132.htm

DOI: https://dx.doi.org/10.3748/wjg.v28.i26.3132

INTRODUCTION

Gastric cancer (GC) is one of the most prevalent gastrointestinal tumors and the third most fatal cancer in the world[1,2]. Additionally, venous thromboembolism (VTE) is a more common complication among GC patients when compared to healthy individuals[3-5]. Notably, VTE is associated with a high mortality in GC patients[6,7]. Several factors, such as tumor stage, neoadjuvant chemotherapy, and surgery, contribute to the development of VTE in GC patients[8,9]. Cancer cells exert a procoagulant activity (PCA) in their microenvironment, which is related to activation of the coagulation system[10]. However, the molecular mechanism underlying PCA in GC patients is poorly understood. Uncovering molecular targets associated with VTE in GC patients can help in the development of appropriate therapy, which can improve the clinical outcomes of these patients.

Neutrophil extracellular traps (NETs) are web-like structures composed of filamentous DNA and histones, decorated with antimicrobial protein granules and enzymes, including neutrophil elastase (NE), myeloperoxidase (MPO), matrix metalloproteinase-9 (MMP-9), and cathepsin G (CatG)[11,12]. They result from interactions between neutrophils and bacterial or other stimulating factors[13,14]. Overall, they protect the host from pathogen-related damage. NETs were initially described as an antimicrobial reaction, but some undesirable effects of NETs have been reported in autoimmune diseases[15-17]. Citrullinated histone H3 (citH3) is proposed as a biomarker reflecting NETs formation. Recent studies have linked NETs to the development of metastasis and cancer-associated thrombosis[18,19]. In particular, NETs result in arterial and venous thrombosis, both of which are mediated by neutrophils[20]. Furthermore, using mouse models, it has been shown that thrombosis in breast cancer tissues is closely linked to the formation of NETs[21]. This finding suggests the potential relationship between NETs and cancer-associated thrombosis.

A recent study revealed that priming metastatic pancreatic cancer cells with platelets stimulates neutrophils to release NETs, which promotes thrombosis in both static and dynamic states[22]. We first reported that platelets derived from GC can stimulate neutrophils to release NETs. NETs enhance PCA in GC patients, which is positively correlated with the expression of the thrombin–antithrombin (TAT)

complex and the level of serum D-dimers[23]. Moreover, both human and animal studies suggest that enhanced thrombosis may result from increased activated platelets[24,25]. Nevertheless, little is known about the interaction between NETs and platelet activation in GC patients. Venous endothelial cell (EC) injury in cancer patients is also closely related to venous thrombosis[26,27]. Interestingly, the cytotoxicity of NETs against ECs enhances PCA in oral squamous cancer, even in patients with obstructive jaundice and inflammatory bowel disease[28-30]. Even so, the potential mechanism underlying EC injury in GC patients is poorly understood.

Our central hypothesis is that GC-induced NETs participate in VTE responses by platelet activation and endothelial injury. Therefore, we first explored the complex relationship between NET formation and platelet activation as well as EC injury. Furthermore, we showed the effect of NETs on thrombosis in an inferior vena cava (IVC) stenosis mouse model. In general, our results may indicate that NETs are potential therapeutic targets in the prevention and treatment of VTE in GC patients.

MATERIALS AND METHODS

Patients and tissue samples

Sixty-three patients newly diagnosed with primary GC and 13 healthy donors (HDs) attending the Second Affiliated Hospital of Harbin Medical University between October 2019 and April 2021 were enrolled in this study. GC diagnoses were performed based on pathological examinations. Pathological tumor-node-metastasis (TNM) staging and histological classification of GC were performed according to the 7th American Joint Committee on Cancer (AJCC) guidelines[31]. Patients who were < 18 years old or pregnant, those on antitumor or anticoagulant treatment before surgical treatment, or those with underlying complications such as endocrine, cardiovascular, hematological and other cancers or infectious disease were all excluded. The main clinical characteristics of the patients with GC and HDs are shown in Table 1. We extracted tumor and adjacent normal tissues from GC patients who consented to this study in writing. Blood samples of preoperative patients were obtained at first diagnosis before any clinical treatment, and blood samples of postoperative patients were obtained from 1 mo after surgery before adjuvant therapy to avoid errors caused by postoperative stress. The protocol for this study was approved by the Ethics Committee of the Second Affiliated Hospital of Harbin Medical University (No. KY2016-032).

Isolation of human plasma, platelets, and neutrophils

Fresh whole venous blood was collected into tubes containing 3.2% sodium citrate using 21-gauge needles. The patients underwent overnight fasting before blood collection. The blood was centrifuged at 150 *g* for 20 min at room temperature (RT) to obtain platelet-rich plasma (PRP), within 1 h of collection. Clean top PRP layer was collected in a new tube, diluted with platelet wash buffer (TBD, Tianjin, China), and centrifuged at 460 *g* for 20 min at RT to obtain clean platelets and platelet-free plasma (PFP) [32]. The platelets were resuspended in prewarmed modified Tyrode's buffer (137 mmoL/L NaCl, 2.8 mmoL/L KCl, 1.0 mmoL/L $MgCl_2$, 12 mmoL/L $NaHCO_3$, 0.4 mmoL/L Na_2HPO_4, 5.5 mmoL/L glucose, pH 7.4; Solarbio, Beijing, China). Neutrophils were isolated based on the density gradient centrifugation, using the whole blood neutrophil isolation kit (TBD). After lysing erythrocytes based on the red blood cell lysis buffer (150 mmoL/L NH_4CL, 10 mmoL/L $KHCO_3$, 0.2 mmoL/L Na_2EDTA, pH 7.4; TBD), the purity (> 96%) and viability (> 96%) of neutrophils were assessed using Wright–Giemsa staining and Trypan blue staining, respectively.

Cell lines and conditioned medium

The human metastatic GC KATO-III and MKN-45 cell lines, human primary GC AGS cell line, human gastric mucosal epithelial cell (GES-1) line, human umbilical cord endothelial cell (HUVEC) line, and mouse forestomach squamous carcinoma (MFC) cell line were purchased from PROCELL (Wuhan, China). All cell lines were characterized using short tandem repeat (STR) profiling. The GES-1, AGS, MKN-45 and MFC cells were cultured in RPMI 1640 (Gibco, USA), KATO-III cells were cultured in IMDM (Gibco), and HUVECs were cultured in DME/F12 (HyClone, Logan, UT, USA). All media were supplemented with 10% fetal bovine serum (FBS; Gibco) and 1% penicillin–streptomycin solution (Beyotime, Beijing, China). Incubation was performed at 37°C under 5% CO_2in a humidified environment. To prepare conditioned medium (CM), the cells were cultured to 90% confluence in medium supplemented with 10% FBS, washed three times using 1 × PBS, and recultured for 48 h in medium without FBS. The supernatant was centrifuged at 1500 *g* for 10 min at 4°C to remove cell debris. The CM was collected and stored at -80°C until use.

Animal models

The animal protocol was designed to minimize pain or discomfort to the animals. Wild-type male C57BL/6 mice (7–9 wk old, weighing 20–26 g) were purchased from the Animal Experimental Center of Harbin Medical University, and all procedures were approved by the Animal Care and Use Committee

Table 1 Main clinical and laboratory features of 13 healthy subjects and 63 patients diagnosed with gastric cancer

Characteristics (n = 76, DF = 4)	Control (n = 13)	Stage I (n = 14)	Stage II (n = 15)	Stage III (n = 22)	Stage IV (n = 12)
Male (%)	61.5	50	53.3	72.7	66.6
Age(yr)	58.46 ± 5.43	57.0 ± 10.07	63.07 ± 9.12	60.32 ± 11.54	63.64 ± 9.68
Erythrocytes (× 10^{12}/L)	4.70 ± 0.57	4.46 ± 0.32	4.12 ± 0.83	4.13 ± 0.69	4.03 ± 0.81
Leukocytes (× 10^{9}/L)	6.87 ± 2.86	6.57 ± 2.04	8.60 ± 2.54[a]	8.58 ± 4.66[a]	10.60 ± 5.25[b]
Neutrophils (× 10^{9}/L)	4.36 ± 3.0	4.62 ± 2.54	6.36 ± 2.82[a]	6.75 ± 4.92[a]	8.53 ± 5.46[c]
Hb (g/L)	140.84 ± 20.31	137.23 ± 10.76	121.29 ± 26.65	121.23 ± 29.72	111 ± 33.23[a]
PLT (× 10^{9})	259.15 ± 59.0	242.69 ± 52.19	293.29 ± 83.74	250.64 ± 104.63	302.0 ± 156.9
ALB (g/L)	44.84 ± 3.27	43.33 ± 4.84	38.06 ± 6.29	37.39 ± 9.23	35.59 ± 4.08[a]
PT (s)	11.24 ± 1.03	12.66 ± 4.16	12.42 ± 2.03	12.05 ± 0.86	12.24 ± 1.57
APTT (s)	35.06 ± 2.71	36.03 ± 7.54	34.52 ± 3.46	33.49±3.81	35.08±4.68
D-dimer (mg/L)	53.30 ± 48.16	238.46 ± 265.28[c]	280.21 ± 269.55[c]	291.23 ± 262.88[c]	950.0 ± 743.72[d]
Fibrinogen (g/L)	2.46 ± 0.43	2.69 ± 0.58	3.67 ± 0.98[a]	3.19 ± 0.61[a]	4.68 ± 2.61[b]

[a]P < 0.05 *vs* healthy control.
[b]P < 0.01 *vs* healthy control.
[c]P < 0.001 *vs* healthy control.
[d]P < 0.0001 *vs* healthy control.
Data are presented as numbers (percentages) or the mean ± SD. DF: Degree of freedom; Hb: Hemoglobin; PLT: Platelets; ALB: Albumin; PT: Prothrombin time; APTT: Activated partial thromboplastin time.

of the Second Affiliated Hospital of Harbin Medical University (No. KY2016-032). The animals were individually housed and maintained under standard conditions (12 h/12 h light/dark cycle, 22 ± 1 °C, 50% humidity) and provided with a conventional laboratory diet and an unrestricted supply of drinking water. In the subcutaneous tumor models, mice were injected with MFC cells (2 × 10^{7} cells/mL) subcutaneously into the right axilla, and the tumor volumes were measured every 3 d from 7 d after injection with MFC cells and allowed to reach 1000 mm^{3} (usually 28–35 d). The volume was calculated by measuring the length (L) and width (W) of the tumor: Tumor volume = π/6 × L × W^{2}. Thereafter, a murine model of deep vein thrombosis (DVT) was developed as previously described[33]. The mice were anesthetized by intraperitoneal injection of 2,2,2-tribromoethanol (Sigma, St . Louis, MO, USA), and the intestines were removed to expose the IVC after entering the abdominal cavity through a median abdominal incision. The IVC was carefully separated below the left renal vein plane. After 5-0 (1 mm) sutures passed through the IVC, 3-0 (2 mm) sutures were placed at the parallel part of the IVC as the blocking line. The IVC was ligated and 3-0 sutures were carefully extracted. This procedure has been shown to decrease the vascular lumen by approximately 90%. The other branches of the IVC were ligated to the level of the iliac vein. Thereafter, the abdominal incision was closed, mice were sacrificed after 6 or 48 h, and thrombi that had formed in the IVC were harvested. The IVC stenosis mice in the treatment groups were injected with DNase I (50 μg/mouse; Roche, Switzerland) intraperitoneally every 12 h until the time of death. All animals were killed for tissue collection. Blood (300 μL/mouse) was drawn from the periorbital eye plexus and stabilized with 0.5 mmoL/L EDTA. Plasma was obtained as described above. Thrombi of control and tumor-bearing mice were fixed in 4% paraformaldehyde for 24 h, embedded in Optimal Cutting Temperature (OCT) compound (SAKURA, Torrance, CA, USA), and cryosectioned at a thickness of 4 μm for immunofluorescence staining.

Quantification of plasma NETs marker

Plasma cell-free DNA (cf-DNA), MPO-DNA and citH3-DNA complexes were quantified using capture ELISA as previously described[34]. The quantification of cf-DNA was performed using the Quant-iT PicoGreen dsDNA assay kit (Invitrogen, Carlsbad, CA, USA). For detection of NET-DNA complexes, 5 μg/mL anti-MPO (ab90810; Abcam, Cambridge, UK) or anti-citH3 antibody (ab5103; Abcam) was coated onto 96-well plates overnight at 4°C. After blocking in 1% bovine serum albumin (BSA), the plasma from GC patients or healthy individuals was added per well and incubated at RT for 2 h. After washing five times with PBST, Quant-iT PicoGreen dsDNA Reagent was added. The values were then read with a fluorometer with a filter setting of 480 nm/520 nm excitation/emission wavelengths.

Fibrin formation and TAT complex assay

Fibrin formation of platelets and ECs was detected by turbidity as previously described[35]. To assess

the fibrin formation in the setting of platelet or EC monolayers, cell monolayers in 96-well plates were stimulated by NETs with or without DNase I, activated protein C (APC), and sivelestat treatment alone or together for 4 h, followed by two washes with Hank's balanced salt solution (137 mmoL/L NaCl, 5.3 mmoL/L KCl, 4.17 mmoL/L $NaHCO_3$, 0.33 mmoL/L Na_2HPO_4, 5.5 mmoL/L glucose, pH 7.4) and then 150 μL PFP from HDs was cocultured with cells at 37°C for 2 min, followed by the addition of 50 μL prewarmed 25 mmoL/L $CaCl_2$. The fibrin formation was tested using turbidity measurements and quantified as the maximum value by measuring the OD at 405 nm every 10 s for 30 min on a SpectraMax 340 PC plate reader. To assess the fibrin formation in the plasma of mice, 150 μL PFP from control, tumor-bearing mice, or DNase I infused tumor-bearing mice was cultured at 37°C for 2 min, followed by addition of 50 μL prewarmed 25 mmoL/L $CaCl_2$. To detect the level of TAT complex, a human and mouse TAT complex ELISA kit (Jingkbio, Shanghai, China) was used as previously described[36].

Flow cytometry

Circulating NETs were measured using flow cytometry. Here, whole blood from HDs and GC patients was diluted with 1 × PBS and incubated in the dark at RT for 30 min with FITC-conjugated-citH3 (eBioscience, San Diego, CA, USA) and PE-conjugated MPO (eBioscience) antibodies. For the assessment of phosphatidylserine (PS) and P-selectin expression on platelets, platelets (2×10^6 cells) isolated from the blood of HDs and GC patients were incubated with FITC-conjugated lactadherin (Haematologic, Essex Junction, VT, USA), APC-conjugated CD62P (Biolegend, San Diego, CA, USA), and PerCP-conjugated CD41 (Biolegend) antibodies.

Immunofluorescence staining of NETs

Tumor and paratumor tissues of GC patients were fixed in 4% paraformaldehyde for 24 h, embedded in OCT compound (SAKURA), and cryosectioned into slices of 4-μm thickness. The samples were cultured overnight at 4°C with primary rabbit anti-histone H3 (1:500, ab5103; Abcam) and mouse anti-MPO (1:500, ab90810; Abcam) antibodies, and washed three times with PBS before incubation for 1 h at RT with Alexa Fluor 594-conjugated goat anti-rabbit (1:200; Proteintech, China) and Alexa Fluor 488-conjugated goat anti-mouse (1:200; Proteintech) secondary antibodies. The tissues were stained for 5 min at RT in the dark with 4',6-diamidino-2-phenylindole (DAPI) and anti-fade mounting medium (Solarbio, Beijing, China). Thrombi in the IVC of tumor models or control mice were stained with primary rabbit anti-histone H3 (1:500, ab5103; Abcam) and rat anti-Ly6G (1:500, Novus, St. Charles, MO, USA), and the specimens were incubated with the Alexa Fluor 488-conjugated goat anti-rabbit (1:200; Proteintech) and Alexa Fluor 594-conjugated goat anti-rat (1:200; Proteintech) secondary antibodies as previously described[37]. The tissue images were captured using a confocal microscope (LSM 800; Zeiss, Germany).

Neutrophils (5×10^5 cells) isolated from HDs were seeded and incubated in glass-based poly-L-lysine-coated 24-well plates for 1 h at 37°C under 5% CO_2. Thereafter, cell suspensions of KATO-III, MKN-45, AGS, and GES-1 (2×10^5 cells) or CM from GC cells were cocultured with neutrophils for 4 h at 37°C under 5% CO_2. To detect and quantify NETs, the samples of the CM group were incubated with primary rabbit anti-histone H3 and mouse anti-MPO antibodies and then fluorescent secondary antibodies. For the samples of cell-cell contact groups, NETs were stained with Sytox Green (Solarbio) for 10 min in the dark at RT. All images were captured using a confocal microscope (LSM 800; Zeiss) and analyzed with ImageJ software (National Institutes of Health, Bethesda, MD, USA).

Preparation of cell-free NETs

Cell-free NETs were isolated from neutrophils of GC patients as previously described, with modifications[38]. Neutrophils (10^7 cells/mL) were cultured for 4 h at 37°C under 5% CO_2 in medium supplemented with 500 nM PMA (HY-18739; MedChemExpress, Monmouth Junction, NJ, USA). The supernatant was discarded, and ice-cold 1 × PBS was added to wash down the cell layer of neutrophils to obtain the NET medium and centrifuged at 1500 *g* for 10 min at 4°C to remove cell debris. Thereafter, 1.5 mL supernatant (sterile DNA–protein complex) was centrifuged at 15 000 *g* for 15 min at 4°C. The resultant pellets were suspended in ice-cold 1 × PBS, followed by DNA concentration measurement in the medium obtained using spectrophotometry (Biospec-nano, Japan). An adequate DNA concentration in the medium should range between 50 and 100 μg/mL. The medium containing the NETs was stored at -80°C for subsequent experiments.

Platelet activation and adhesion assays

Platelet activation and adhesion assays were performed as previously described[22]. Glass-based wells of 24-well plates were coated with cell-free NETs after overnight incubation in the corresponding medium at 4°C in a humidified chamber. For controls, 1% denatured BSA was used. Denatured BSA was prepared by heating the solution in PBS without calcium or magnesium to 80°C for 3 min and immediately placing it on ice until cool; it was then stored at 20°C until use. Platelet suspensions (10^7 cells/mL) were then seeded in the wells, cultured for 1 h at 37°C under 5% CO_2, fixed for 15 min at RT with 4% paraformaldehyde, and washed three times using 1 × PBS before 20 min permeabilization

using 0.1% Triton-X 100. The platelets were then incubated for 30 min with Alexa Fluor 594-conjugated phalloidin primary antibody (1:300; Thermo Fisher, Waltham, MA, USA). To assess PS and P-selectin expression, the platelet suspension was incubated for 1 h at 37°C under 5% CO_2, and the cells were stimulated with NETs for 1 h, followed by FITC-conjugated lactadherin (Hematologic) staining for 30 min. Platelets were washed twice with PBS before fixation for 15 min at RT with 4% paraformaldehyde, permeabilized using 0.1% Triton-X 100 for 20 min, and then stained with primary rabbit anti-P-selectin (1:200; Proteintech) and mouse anti-CD41 (1:500; Novus) antibodies. Images were captured using a confocal microscope (LSM 800; Zeiss) and analyzed with ImageJ software (National Institutes of Health).

HUVECs stimulation assay

HUVECs were incubated with cell-free NETs or PBS in 24-well plates for 4 h when the cells grew to a confluent monolayer. The cells were fixed in 4% paraformaldehyde for 15 min at RT, washed three times using 1 × PBS, and blocked for 1 h using 10% goat serum with 1% BSA solution in PBS. For detection of tissue factor (TF) expression, ECs were incubated overnight at 4 °C with rabbit anti-TF (1:500, ab228968; Abcam) and mouse anti-CD31 (1:500, ab9498; Abcam) primary antibodies. The cells were washed with PBS and reincubated for 1 h at RT with Alexa Fluor 594-conjugated (Proteintech) goat anti-rabbit and Alexa Fluor 488-conjugated (Proteintech) goat anti-mouse secondary antibodies. For detection of intercellular junctions of cells, cells were incubated overnight at 4°C with rabbit anti-VE-cadherin (1:500, ab33168; Abcam) primary antibody, followed by Alexa Fluor 488-conjugated (Proteintech) goat anti-rabbit secondary antibody, and were further incubated with Alexa Fluor 594-conjugated phalloidin primary antibody (1:300; Thermo Fisher, Waltham, MA, USA). They were stained with DAPI and fixed with mounting medium (Solarbio) for 5 min at RT in the dark. The cells were observed and photographed using a confocal microscope. The photos were analyzed with ImageJ software.

Platelet and HUVEC inhibition assays

For inhibition assays, platelets and HUVECs were cocultured with cell-free NETs for 1 h at 37°C in a humidifier chamber in the presence of DNase I (100 U/mL, Roche), APC (100 nM, HY-P1918; MedChemExpress), and sivelestat (100 nM, HY-17443; MedChemExpress) alone or together. DNase I cleaves NET DNA, whereas APC and sivelestat disrupt histones and NE functions, respectively.

Statistical analysis

Data are expressed as the mean ± SD. Data were analyzed to assess distribution normality. For normally distributed data, statistical significance was analyzed using Student's *t*-tests and one-way analysis of variance. For non-normally distributed data, statistical significance was analyzed using the Mann–Whitney test and Kruskal–Wallis test. All analyses were performed using GraphPad Prism version 8.0 and SPSS 16.0 statistical software. Spearman's correlation was used to evaluate the association between two variables. $P < 0.05$ was considered statistically significant.

RESULTS

GC patients display greater NET formation

The levels of plasma cf-DNA, citH3-DNA,and MPO-DNA complexes in GC patients ($n = 63$) and HDs ($n = 13$), which reflect the concentration of NETs, were measured using capture ELISA. The levels of NET markers were significantly higher in patients with stage II/III/IV GC than in HDs (Figure 1A–C). There was also a significant difference in preoperative and postoperative plasma NET marker levels in GC patients (Figure 1D–F). The levels of NET markers positively correlated with those of serum D-dimer (cf-DNA: $r = 0.5595$, $P < 0.0001$; citH3-DNA: $r = 0.5469$, $P < 0.0001$; MPO-DNA: $r = 0.5479$, $P < 0.0001$), suggesting that NETs were associated with hypercoagulation and VTE development in GC patients. The levels of NETs ($MPO^+/citH3^+$ neutrophils) in the circulation in GC patients and HDs were measured using flow cytometry. Circulating NETs were higher in the blood of patients with either GC stage (II–IV) than in their HD counterparts (Figure 1G and H). Furthermore, based on MPO and citH3 levels, immunofluorescence staining revealed that NETs were significantly higher in the tumor microenvironment than in the paratumor tissue of the same patients (Figure 1I–M).

GC cells stimulate formation of NETs by neutrophils

To assess whether GC cells directly stimulated NET formation, we analyzed the expression of NETs in a coculture of GC cell lines and neutrophils. Immunofluorescence analysis revealed that compared with GES-1 cells, the rate of NET formation was significantly higher in GC cells (Figure 2A). However, the formation of NETs was greater in the metastatic GC cell line than in the nonmetastatic GC cell line (Figure 2B). We measured NET formation when normal neutrophils were cocultured with CM from KATO-III, MKN-45, AGS and GES-1 cells. Immunofluorescence analysis further revealed that the CM of KATO-III and MKN-45 cells exerted greater neutrophil activation for NET formation than the CM of

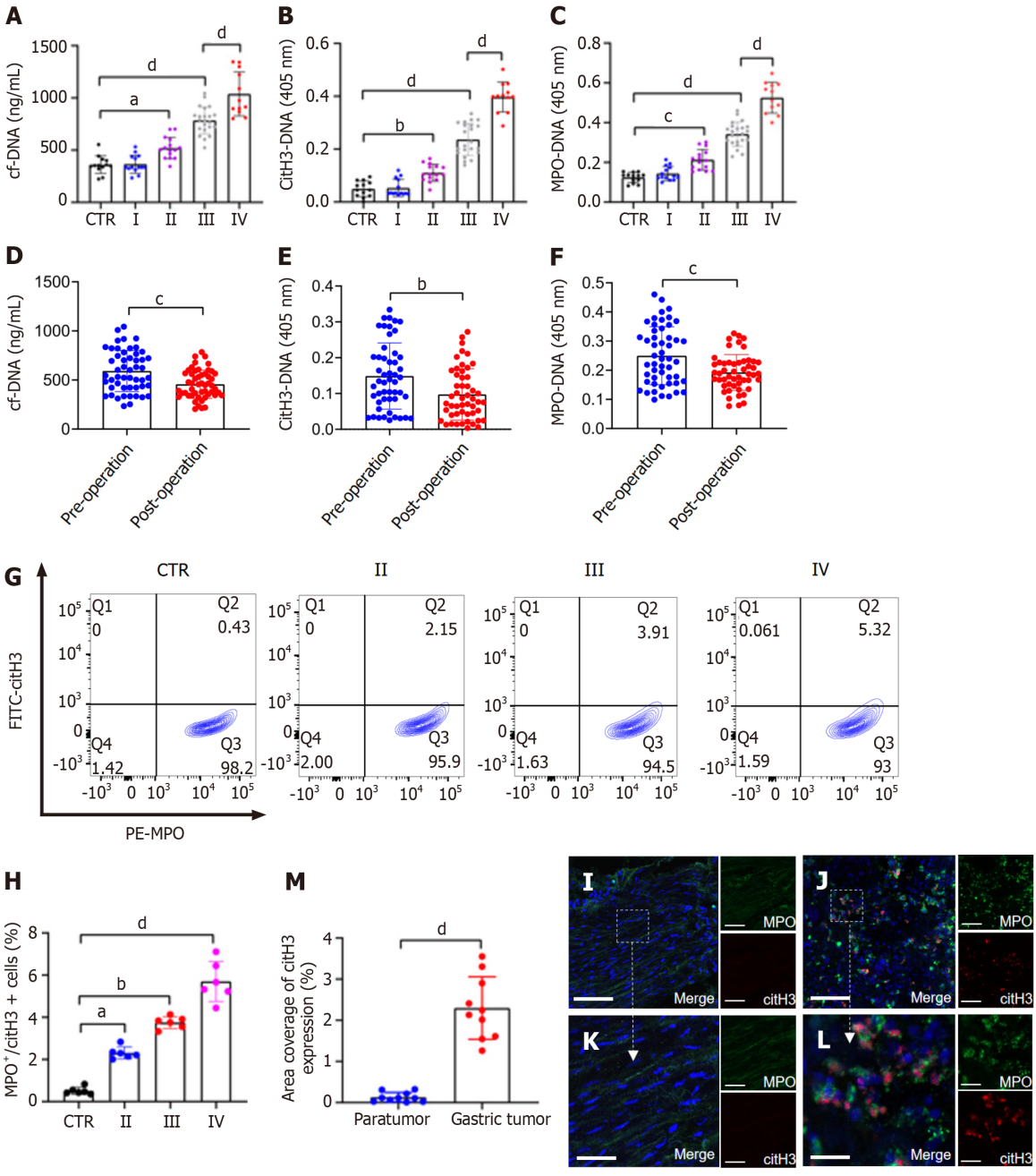

DOI: 10.3748/wjg.v28.i26.3132

Figure 1 NETs are accumulated in samples of GC patients. A–C: Plasma levels of NET markers cf-DNA, citH3-DNA, and MPO-DNA in GC patients and healthy individuals were measured by ELISA. Healthy individuals, *n* = 13; stage I, *n* = 14; II, *n* = 15; III, *n* = 22; IV, *n* = 12; D-F: Comparison of cf-DNA, citH3-DNA and MPO-DNA in the plasma of patients with GC preoperatively and postoperatively by ELISA. *n* = 51; G and H: The rate of activated neutrophils in the circulating environment of GC patients and healthy individuals was measured by flow cytometry with APC-MPO and FITC-citH3 staining. Each group: *n* = 6; I and J: NET accumulation was detected by confocal microscopy with MPO and citH3 staining in paratumor and tumor samples from the same GC patient. Magnification 20×; scale bars: 50 μm. Red-citH3, Green-MPO and Blue-DAPI; K and L: Magnified (40×) part of MPO and citH3 colocation in paratumor and tumor samples from the same patient. Scale bars: 10 μm. Red-citH3, Green-MPO and Blue-DAPI; M: The percentage of area coverage of citH3 expression was defined as the rate of red area in total area and analyzed with ImageJ software; all values are the mean ± SD. $^{a}P < 0.05$; $^{b}P < 0.01$; $^{c}P < 0.001$; $^{d}P < 0.0001$. NET: Neutrophil extracellular trap; GC: Gastric cancer; cf-DNA: Cell-free DNA; MPO: Myeloperoxidase; citH3: Citrullinated histone H3.

AGS cells. However, the CM of GES-1 cells had no effect on NET formation (Figure 2C and D). Overall, these findings demonstrate that GC cells stimulate NET formation through both intercellular contact and noncontact mechanisms.

NETs contribute to hypercoagulation of platelets

To examine the effect of NETs on platelet activation, we measured the levels of PS and P-selectin expression in these cells. Flow cytometry revealed that compared to HDs, the expression of PS and P-selectin was significantly higher on platelets of patients with GC (Figure 3). In addition, platelets

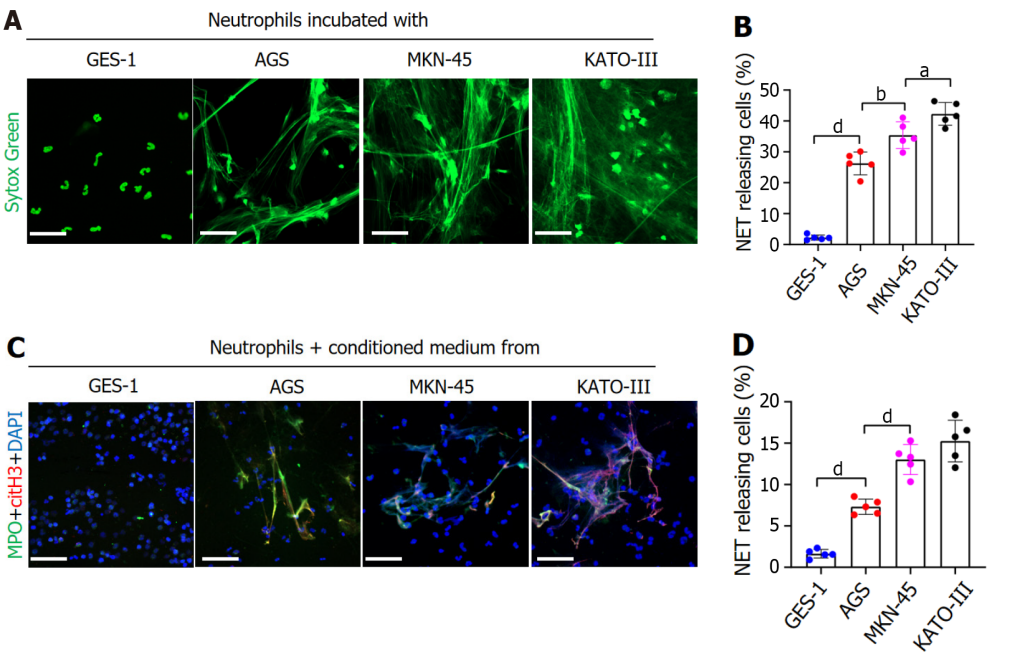

DOI: 10.3748/wjg.v28.26.3132

Figure 2 GC cells can stimulate neutrophils to form NETs. A and B: Control neutrophils were cocultured with normal gastric mucosal epithelial cells (GES-1) or GC cells (AGS, MKN-45 and KATO-III) and NET formation was measured by confocal microscopy with cell-impermeable Sytox-Green staining. Magnification 20×; scale bars: 50 μm. Green: Neutrophils; C and D: Control neutrophils were cocultured with CM from GES-1 or GC cells, and stained with MPO and citH3. The percentage of NET-releasing cells was defined as the ratio of the calculated NET releasing neutrophils to the total number of neutrophils. Magnification 20×; scale bars: 50 μm. Red-citH3, Green-MPO, and Blue-DAPI. All values are the mean ± SD. $^{a}P < 0.05$; $^{b}P < 0.01$; $^{c}P < 0.001$; $^{d}P < 0.0001$. GC: Gastric cancer; GES-1: Gastric mucosal epithelial cells; NET: Neutrophil extracellular trap; CM: Conditioned medium; MPO: Myeloperoxidase; citH3: Citrullinated histone H3.

isolated from HDs were cocultured with NET medium or PBS before analyzing PS and P-selectin expression. We found that NETs stimulated PS and P-selectin expression on platelets by confocal microscopy (Figure 4A–C). Flow cytometry also demonstrated this hypercoagulable phenotype of platelets which was stimulated by NETs (Figure 4D and E). In the inhibition assay, we added DNase I, APC and sivelestat alone or together to cleave DNA, histones and NE, which were the most functional factors of NETs. At the highest concentration of NETs (0.5 μg DNA/mL), flow cytometry revealed that DNase I, APC, sivelestat, or a combination of the three inhibited 60.2%, 47.1%, 41.9% and 83.2% of PS expression, respectively (Figure 4D), and 55.2%, 47.0%, 41.0%, and 91.76% of P-selectin expression on platelets, respectively (Figure 4E).

NETs promote platelet adhesion and prothrombotic state

Previous studies have shown that NETs promote thrombosis in murine late-stage breast cancer models and DVT models[19,39]. However, whether NETs derived from GC neutrophils have the ability to stimulate platelet adhesion under static conditions is unknown. To determine the effect of NETs on platelet adhesion, platelets isolated from HDs were seeded in NET-coated wells to measure the effects of NETs on the adherence of platelets to blood vessels. Confocal microscopy revealed that NETs enhanced adherence of platelets to glass slides (Figure 5A and B), indicating that NETs induce the development of thrombosis. Moreover, the results revealed that fibrin formation and TAT complex levels were increased when control plasma was cocultured with platelets activated by NETs (Figure 5C and D).

Inhibition assays revealed that digestion of NET DNA using DNase I modulated the adhesion of platelets on glass surfaces. Even so, a few platelets still adhered to the NET-coated well pretreated with DNase I (Figure 5A). This suggested that other protein components other than NET-DNA participated in the adhesion of platelets. NETs treated with DNase I, APC, sivelestat, or a combination of the three inhibited 67.1%, 56.6%, 38.9%, and 91.8% of platelet adhesion, respectively (Figure 5B). The degree of platelet adhesion in the combination group was comparable to that of the controls. We found that DNase I, APC, sivelestat, or a combination of the three reduced fibrin formation by 81.1%, 73.9%, 64.3%, and 90.7%, respectively (Figure 5C), and inhibited 78.9%, 57.4%, 51.2%, and 91.9% of TAT complex level, respectively (Figure 5D), at the highest concentration of NETs. Taken together, these findings demonstrate that NETs play a role in the development of thrombosis.

NETs drive hypercoagulation of ECs

To detect the effect of NETs on EC thrombogenicity, HUVECs were cocultured with NET medium. Confocal microscopy revealed that NETs destroyed the normal intercellular junctions between ECs

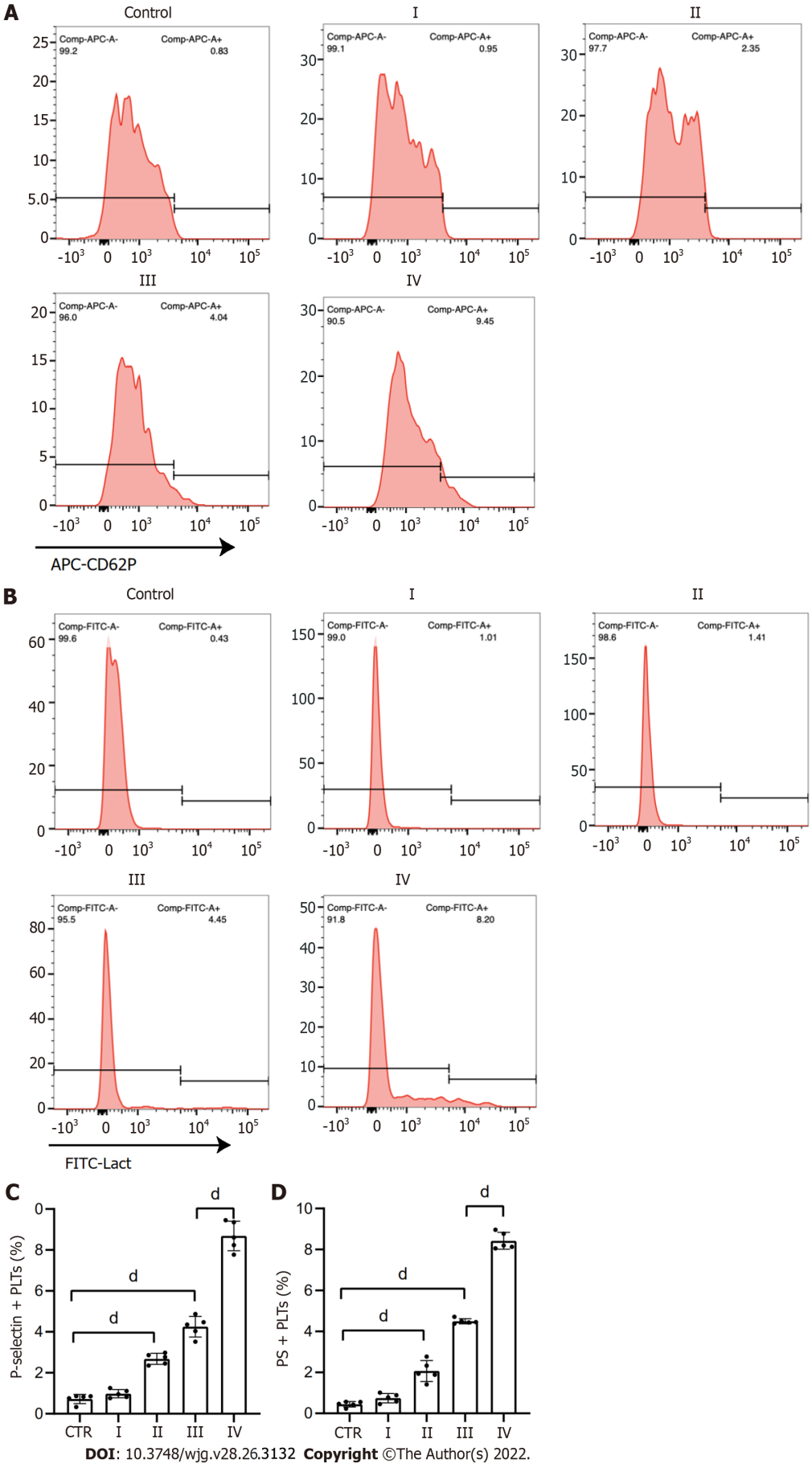

DOI: 10.3748/wjg.v28.26.3132

Figure 3 Platelets are activated in patients with GC. A and C: Flow cytometry showed the rate of P-selectin-positive platelets from each stage GC patients

and healthy individuals; B and D: Rate of phosphatidylserine-positive platelets from each stage GC patients and healthy individuals. All values are the mean ± SD. $^{d}P < 0.0001$. PS: Phosphatidylserine; GC: Gastric cancer. CD62P: P-selectin; Lact: Lactadherin.

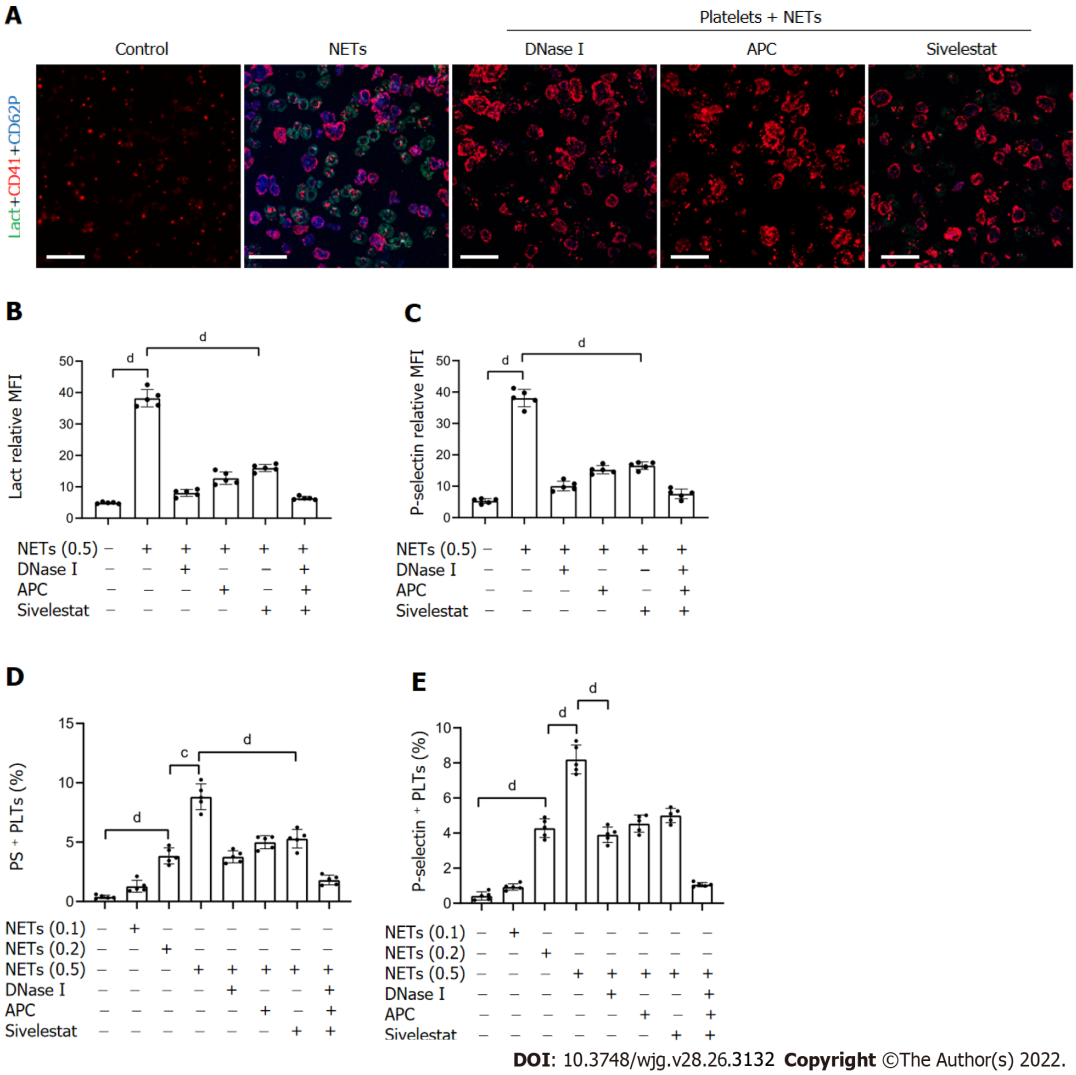

DOI: 10.3748/wjg.v28.26.3132

Figure 4 NETs contribute to hypercoagulation of platelets. A: PS exposure and P-selectin expression were measured when isolated platelets were cocultured with BETs (μg, DNA/mL) or in the presence of DNase I, activated protein C, and sivelestat alone or together by confocal microscopy. Magnification 63×; scale bars: 10 μm. Red-platelets, Green-Lactadherin, and Blue-P-selectin; B and C: PS exposure and P-selectin expression are indicated as MFI. MFI was defined as the ratio of total fluorescence intensity to the area; D and E: The rates of PS-positive platelets and P-selectin-positive platelets were detected by flow cytometry. All values are the mean ± SD. $^{c}P < 0.001$; $^{d}P < 0.0001$. PS: Phosphatidylserine; GC: Gastric cancer; DNase I: Deoxyribonuclease I; APC: Activated protein C; MFI: Mean fluorescence intensity; Lact: Lactadherin; CD41: Platelet; NET: Neutrophil extracellular trap.

(Figure 6A and C). NET treatment upregulated expression of TF on the surface membrane of ECs (Figure 6B and D). In addition, plasma fibrin formation and TAT complex levels were significantly increased when control plasma was incubated with EC monolayers activated by NETs (Figure 6E and F). Further inhibition assays were performed to assess the effect of NETs on ECs after pretreatment with DNase I, APC, sivelestat, or a combination of the three. We found that NET treatment after incubation with DNase I, APC, sivelestat, or all three drugs returned 47.5%, 36.3%, 33.4%, and 86.5%, respectively, of VE expression on ECs (Figure 6C), whereas similar treatment inhibited 60.4%, 44.8%, 38.6%, and 95.5%, respectively, of TF expression (Figure 6D). Additionally, we found that NET treat-ment after incubation with the above inhibitors inhibited 59.7%, 54.4%, 54.0%, and 91.5% of fibrin formation level, respectively (Figure 6E), and inhibited 51.2%, 35.6%, 25.9%, and 84.3% of TAT complex level, respectively (Figure 6F). Taken together, these findings suggest that NETs promote hypercoagulation of ECs; thus, inhibiting NET function can protect against venous injury.

NETs promote formation of thrombi in tumor-bearing IVC flow restriction mice

Based on these findings *in vitro* and the pivotal role of NETs in thrombosis, we hypothesized that GC-

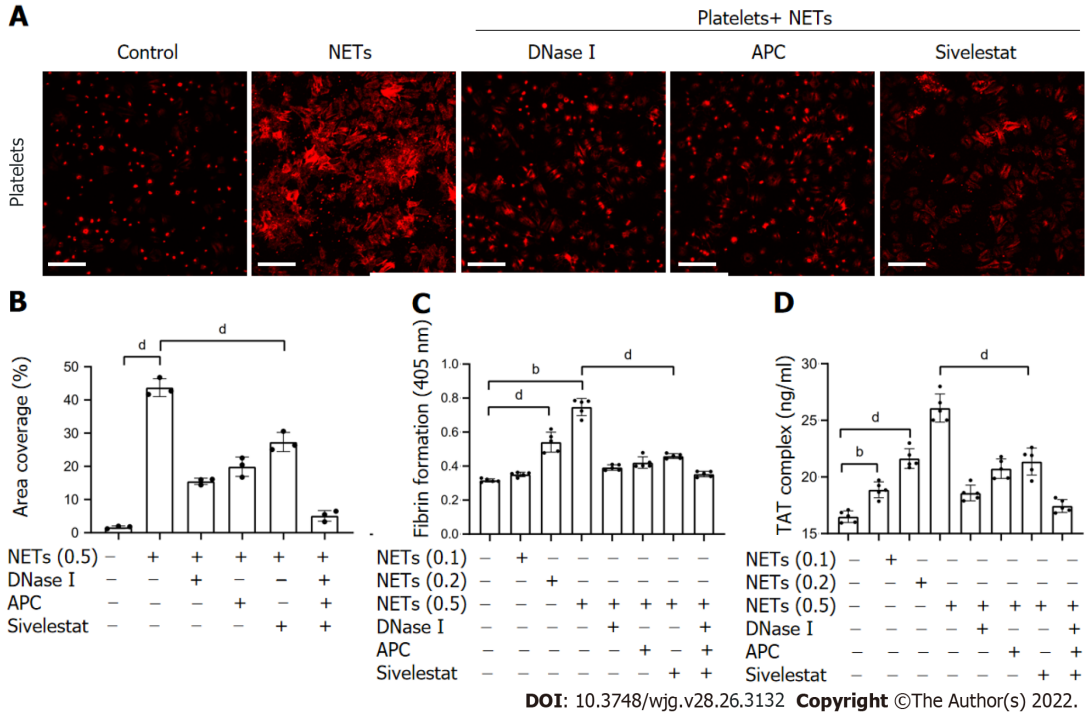

DOI: 10.3748/wjg.v28.26.3132

Figure 5 NETs promote platelet adhesion and prothrombotic state. A: Isolated platelets were incubated on glass slides which were coated with 1% dBSA, NETs (μg DNA/mL), or NETs pretreated with DNase I, APC, and sivelestat alone or together, followed by the F-actin components of platelets with 594-phalloidin staining. Magnification 63×; scale bars: 10 μm. Red-platelets; B: The percentage of area coverage of platelet adhesion was defined as the rate of red area in the total area and analyzed with ImageJ software; C: Isolated platelets were cocultured with different concentrations of NETs for 30 min with or without DNase I, APC and sivelestat treatment alone or together, and plasma fibrin formation was tested using turbidity measurements and monitored OD at 405 nm; D: TAT complex level of activated platelets was analyzed by ELISA. All values are the mean ± SD. $^{a}P < 0.05$; $^{b}P < 0.01$; $^{c}P < 0.001$; $^{d}P < 0.0001$. dBSA: Denatured bovine serum albumin; NETs: Neutrophil extracellular traps; DNase I: Deoxyribonuclease I; APC: Activated protein C; TAT: Thrombin–antithrombin.

induced NETs can also promote thrombosis *in vivo*. Here, in a mouse IVC flow stenosis model, tumor-bearing mice demonstrated more capacity to form thrombi and showed heavier weight and longer length of thrombi compared to control mice (Figure 7A–D). In the 6 h models, three of nine of control mice showed thrombi, whereas seven of nine of tumor-bearing mice formed thrombi. In the 48 h models, all mice demonstrated thrombi in the IVC. In addition, confocal images of thrombi formed in the tumor-bearing mice after 48 h of IVC stenosis showed that NETs were significantly accumulated compared to control mice (Figure 7E–H). The thrombi of control mice included some neutrophils (Ly6G+) but were not activated to form NETs (Figure 7E and G). Furthermore, tumor-bearing mice showed higher fibrin formation and TAT complex levels than control mice (Figure 7I and J).

In the inhibition assay, we infused DNase I into mice immediately after IVC stenosis and examined thrombosis after 6 or 48 h of surgery. We found that treatment with DNase I significantly inhibited thrombi formation in tumor-bearing IVC stenosis mice (Figure 7A–D). Furthermore, fibrin formation and TAT complex levels in tumor-bearing mice were significantly decreased by DNase I treatment (Figure 7I and J). These data suggest that NETs play a role in thrombosis *in vivo*, which was induced by GC, and inhibiting NETs by DNase I had a protective effect on thrombosis in this mouse model.

DISCUSSION

Inflammation is one of the hallmarks of cancer. Additionally, neutrophils are among the most important immune cells implicated in promoting tumor progression[40,41]. NETs participate in cancer progression by promoting the proliferation, invasion, metastasis and angiogenesis of cancer cells as well as thrombosis in numerous tumor types[42-44]. A recent study using mouse models with Jak^{2V617F} knock-in revealed that most myeloproliferative neoplasms display NET formation and DVT[45]. Our previous studies revealed that NETs promote the migration and metastasis of GC cells both *in vitro* and *in vivo* through epithelial mesenchymal transition[46]. Intriguingly, inhibition of NETs promotes apoptosis and inhibits the invasion of GC cells by regulating the expression of Bcl-2, Bax and nuclear factor-κB proteins[47]. Our initial studies revealed that NETs released by neutrophils in GC patients promoted the conversion of thrombin and fibrin[23]. Accordingly, we hypothesized that NETs promote thrombosis in GC patients. We investigated the interactions between GC cells, neutrophils, platelets and ECs, with a keen focus on their role in cancer-associated thrombosis.

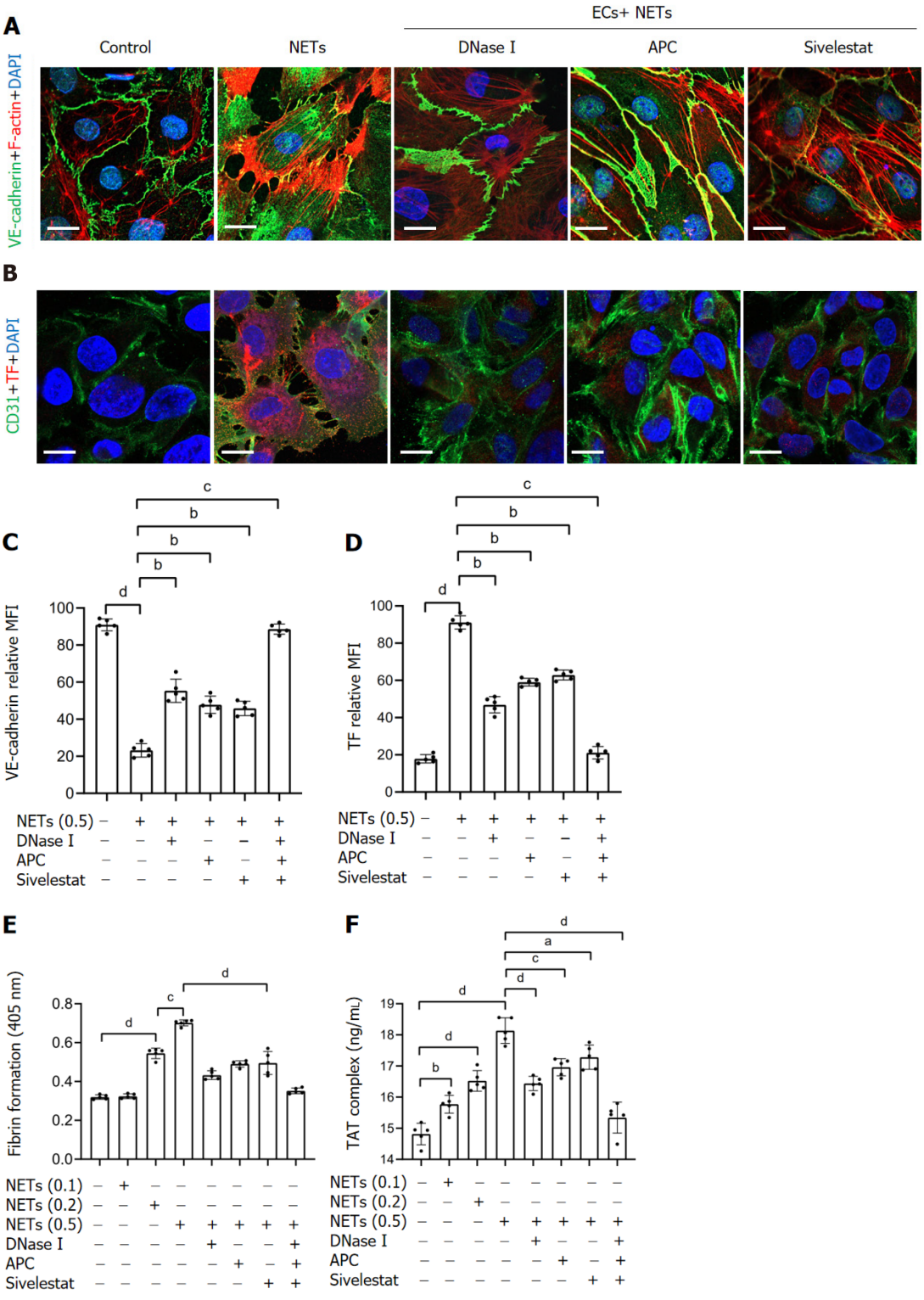

DOI: 10.3748/wjg.v28.26.3132

Figure 6 NETs drive hypercoagulation of ECs. A: ECs were cocultured with NETs (μg DNA/mL) or PBS in the presence of DNase I, APC, or sivelestat alone or together for 4 h and analyzed by confocal microscopy. The intercellular junctions of ECs were stained with VE–cadherin and phalloidin. Magnification 63×; scale bars: 10 μm. Red-phalloidin, Green-VE, and Blue-DAPI; B: EC activation was stained with CD31 and TF. Magnification 63×; scale bars: 10 μm. Red-TF, Green-CD31, and Blue-DAPI; C and D: VE–cadherin expression and TF expression on ECs were detected by confocal microscopy and analyzed with ImageJ software (expression indicated as MFI). MFI was defined as the ratio of total fluorescence intensity to the area; E and F: EC monolayers were stimulated with various concentrations of NETs for 4 h, followed by determination of fibrin formation by turbidity measurement at 405 nm, and the TAT complex level was detected by ELISA. All values are the mean ± SD. $^{a}P < 0.05$; $^{b}P < 0.01$; $^{c}P < 0.001$; $^{d}P < 0.0001$. NETs: Neutrophil extracellular traps; ECs: Endothelial cells; DNase I: Deoxyribonuclease I; APC: Activated protein C; TF: Tissue factor; TAT: Thrombin–antithrombin; MFI: Mean fluorescence intensity.

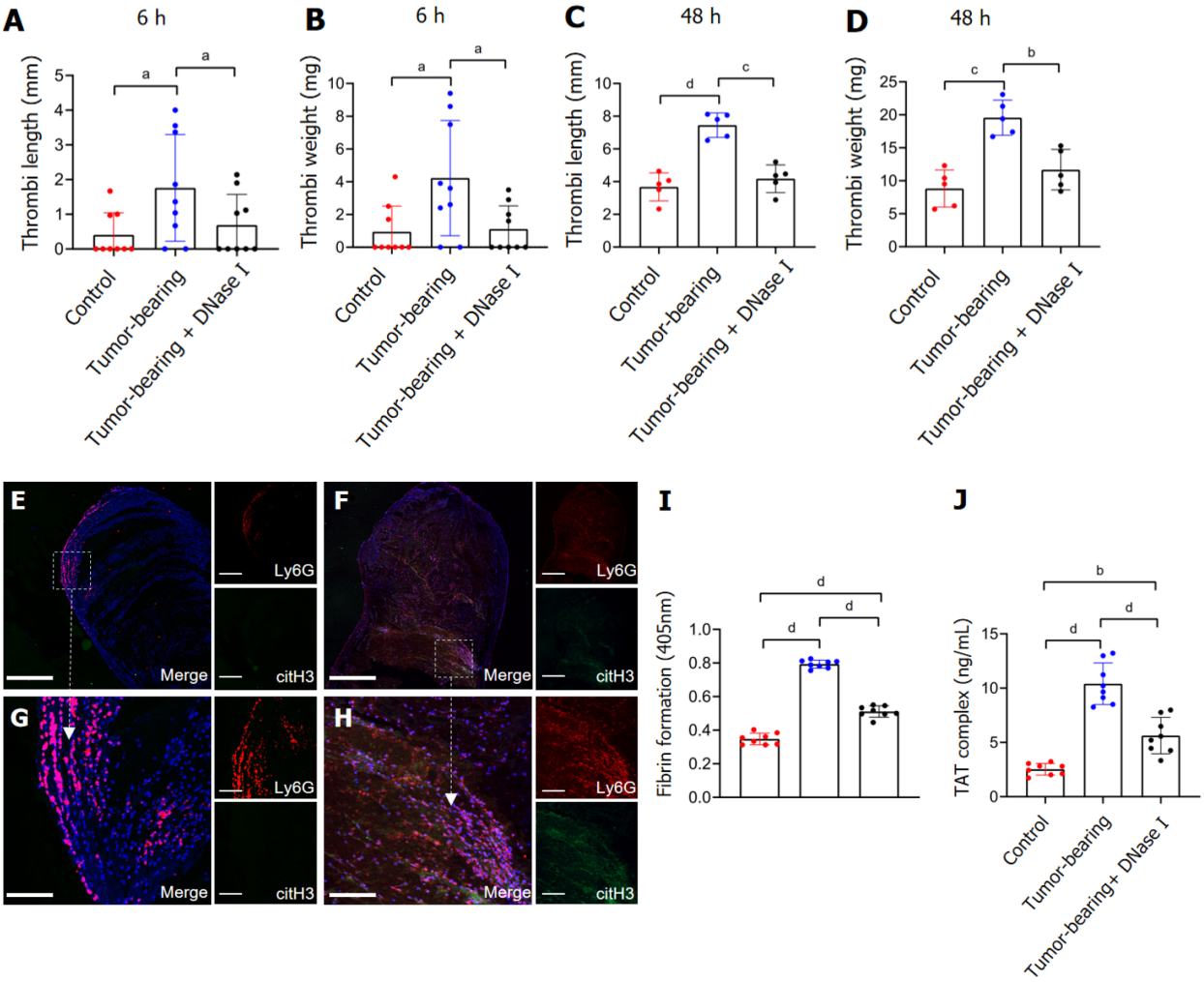

DOI: 10.3748/wjg.v28.i26.3132

Figure 7 Tumor-bearing mice show a greater ability to form thrombi by inferior vena cava flow restriction. A and B: The values for weight and length of thrombi present in control, tumor-bearing mice, DNase I infused tumor-bearing mice at 6 h after surgery. Each group, *n* = 9; C and D: Values for weight and length of thrombi present in mice at 48 h after surgery. Each group, *n* = 5; E and F: Confocal imaging of thrombi derived from control mice and tumor-bearing mice with Ly6G and citH3 staining. Magnification 10×; scale bars: 200 μm. Red-Ly6G, Green-citH3, and Blue-DAPI; G and H: Magnified (40×) part of thrombi derived from control mice and tumor-bearing mice. Scale bars: 50 μm. Red-Ly6G, Green-citH3, and Blue-DAPI; I and J: Fibrin formation levels in the plasma of control, tumor-bearing mice, or DNase-I-infused tumor-bearing mice were detected by turbidity measurement at 405 nm, and TAT complex levels were detected by ELISA. Each group, *n* = 8. All values are the mean ± SD. $^{a}P < 0.05$; $^{b}P < 0.01$; $^{c}P < 0.001$; $^{d}P < 0.0001$. DNase I: Deoxyribonuclease I; TAT: Thrombin–antithrombin.

In this study, we found that the levels of plasma NET markers and citH3-positive neutrophils were significantly higher in GC patients than in HDs. Expression of NETs decreased significantly after resection of GC tissues. Neutrophil infiltration and NET formation were upregulated in tumor tissues, relative to adjacent paratumor tissues of the same GC patient. The levels of serum D-dimer were positively correlated with tumor TNM stage, consistent with previous findings[48]. These findings suggest that the expression of NETs promotes GC development and thrombosis in the same group of patients.

It has been reported that hepatocellular cancer and hypoxic CM stimulate the production of NETs by neutrophils[44]. However, the relationship between GC cells and neutrophils is poorly understood. Our experiments demonstrated that both metastatic and nonmetastatic GC cancer cells directly stimulated production of NETs from neutrophils, contrary to GES-1 cells. CM of GC cells, but not that of GES-1, also induced the formation of neutrophil-related NETs. This suggests that NET formation is also mediated by factors secreted by GC cells. Inflammatory cytokines, such as interleukin (IL)-1β, IL-6, IL-8, and tumor necrosis factor-, as well as damage-associated molecular patterns, all overexpressed in tumor microenvironments, stimulate neutrophils to release NETs[49,50]. Although IL-8 is the cytokine with the highest overexpression in GC patients, whether it is the main mediator of NET formation and the subsequent underlying mechanism in GC remain to be validated.

A recent study showed that NETs promote thrombosis by activating and promoting the adhesion of platelets in the venous walls of pancreatic cancer patients[22]. Activated platelets express PS on their surface membranes[51]. Additionally, P-selectin expression on the surface membrane of platelets is also

associated with thrombosis[52]. In this study, we found that compared to HDs, PS and P-selectin expression on platelets was significantly higher in GC patients, particularly those with stage III/IV GC. NET treatment upregulated PS and P-selectin expression on platelets. Additionally, NETs stimulated the adhesion of normal platelets on glass slides. However, even though DNase I treatment modulated this phenomenon, some platelets still adhered to the glass slides, suggesting that other secretory factors participated in the adhesion property.

Previous studies have shown that histones in NETs promote thrombosis in colorectal cancer patients [53]. NE is another most abundant protein that binds NETs. Although this potent protein stimulates tumor progression both *in vitro* and *in vivo*, the mechanisms underlying NE-mediated cancer-associated thrombosis remain to be clarified. A recent study on DVT using mouse models showed that NE deficiency or NE inhibition alone does not completely inhibit DVT[54]. In this study, we found that hypercoagulation of platelets was not completely mediated by NET DNA, but also by other secretory proteins in the NETs, such as histones and NE. Consequently, DNase I treatment of NETs had no complete effect on hypercoagulation of platelets. However, a combination of DNase I, APC and sivelestat treatment almost completely inhibited hypercoagulation of platelets. Although sivelestat did not show a strong antihypercoagulation effect similar to DNase I, it nonetheless modulated the activation and adhesion of platelets. This demonstrated that histones and NE also participate in the activation and adhesion of platelets.

DVT can be triggered by injury to vascular ECs. Previous studies have shown that under certain malignancies, NETs can induce dysfunction and apoptosis of ECs[35]. In patients with chronic pancreatic disease and pancreatic cancer, NETs exert their cytotoxicity against ECs *via* intercellular cell adhesion molecule-1 and vascular cell adhesion molecule-1 expression[26]. Recent studies have shown that treatment of ECs with NETs derived from patients with colorectal cancer promotes and enhances the production of fibrin and the corresponding coagulation[53]. In this study, we found that NET treatment inhibited the secretion of intercellular junctions in ECs and promoted hypercoagulation of platelets by upregulating TF expression. Moreover, NET treatment upregulated the expression of PS on ECs. ECs activated by NETs significantly increased the level of TAT complexes and fibrin generation in the plasma of HDs. Given that a combination of DNase I, APC and sivelestat treatment completely inhibited hypercoagulation, the process was regulated through numerous mechanisms. These findings strongly suggest that NETs contribute to GC-associated thrombosis.

In the late stage of murine mammary tumor models, thrombi were found in lung vessels, and NETs accumulated, indicating that cancer-induced NETs contribute to the cancer-associated thrombosis[19]. Here, we demonstrated that GC-bearing mice have a greater ability to form thrombi than control mice have and that NETs were abundantly present in the thrombi of tumor-bearing mouse IVC stenosis models. Most of this response can be blocked by DNase I treatment, which was similar to previous studies. In DVT models, flow restriction of the IVC may result in a hypoxic microenvironment to recruit neutrophils and stimulate NET release. In addition, cancer cells often secrete more inflammatory factors, which aggravate the recruitment of neutrophils to form NETs under a hypoxic conditions[50]. Therefore, neutrophils are exposed to two major triggers of NET release: A tumor hypoxic environment and IVC flow restriction, which then participate in the development of thrombi in GC.

CONCLUSION

Our findings demonstrate that GC cells can directly induce NET formation, which in turn strongly increases the risks of VTE development both *in vitro* and *in vivo*. In addition, we found that not only NET DNA but also histones and NE participate in the development of cancer-associated thrombosis. Accordingly, NETs are potential therapeutic targets against VTE in GC patients.

ARTICLE HIGHLIGHTS

Research background

The development of venous thromboembolism (VTE) is associated with high mortality among gastric cancer (GC) patients. Neutrophil extracellular traps (NETs) have been reported to correlate with the prothrombotic state in some diseases, but it was rarely reported in GC patients.

Research motivation

Cancer cells exert a procoagulant activity (PCA) in their microenvironment, which is related to activation of the coagulation system. However, the molecular mechanism underlying PCA in GC patients is poorly understood.

Research objectives

The present study aimed to investigate the effect of NETs on the development of cancer-associated thrombosis in GC patients.

Research methods

The levels of NETs in blood and tissue samples of patients were analyzed by ELISA, flow cytometry, and immunofluorescence staining. NET generation and hypercoagulation of platelets and endothelial cells (ECs) *in vitro* were observed by immunofluorescence staining. NET PCA was determined by fibrin formation and thrombin–antithrombin complex assays. Thrombosis *in vivo* was measured in a murine model induced by flow stenosis in the inferior vena cava (IVC).

Research results

NETs were likely to form in blood and tissue samples of GC patients compared with healthy individuals. *In vitro* studies showed that GC cells and their conditioned medium, but not gastric mucosal epithelial cells, can stimulate NET release from neutrophils. Furthermore, NETs induced hypercoagulable state of platelets and ECs. In a model of IVC stenosis, tumor-bearing mice showed a stronger ability to form thrombi, and NETs abundantly accumulated in the thrombi of tumor-bearing mice compared with control mice. Notably, the combination of deoxyribonuclease, activated protein C, and sivelestat markedly abolished the PCA of NETs.

Research conclusions

Our findings demonstrate that GC-induced NETs strongly increase the risk of VTE development both *in vitro* and *in vivo*. NETs are potential therapeutic targets in the prevention and treatment of VTE in GC patients.

Research perspectives

The treatment strategies can consider the combination of traditional anticoagulant drugs and NETs inhibiting drugs, so as to reduce the risk of cancer associated thrombosis in patients with GC and improve the clinical treatment effect.

FOOTNOTES

Author contributions: Zou XM and Li JC designed the study, completed the experiments, and drafted the manuscript; Yang SF, Zhao TQ, and Jin JQ collected the patient clinical data and performed part of the experiments; Zhu L, Li CJ, and Chen CY participated in the animal experiments; Yang H and Zhang AG performed the statistical analysis; all authors have read and approved the final manuscript.

Supported by National Natural Science Foundation of China, No. 81672355.

Institutional review board statement: The study was reviewed and approved by the ethics committee of the Second Affiliated Hospital of Harbin Medical University (No. KY2016-032).

Institutional animal care and use committee statement: All animal experiments in this study were approved by the ethics committee of the Second Affiliated Hospital of Harbin Medical University (No. KY2016-032).

Conflict-of-interest statement: The authors declare no conflict of interest for this manuscript.

Data sharing statement: No additional data are available.

ARRIVE guidelines statement: The authors have read the ARRIVE guidelines, and the manuscript was prepared and revised according to the ARRIVE guidelines.

Country/Territory of origin: China

ORCID number: Jia-Cheng Li 0000-0002-0467-7225; Xiao-Ming Zou 0000-0002-9689-5026; Shi-Feng Yang 0000-0002-4395-6753; Jia-Qi Jin 0000-0002-7635-5452; Lei Zhu 0000-0002-7495-606X; Chang-Jian Li 0000-0003-0441-0368; Hao Yang 0000-0003-0952-3345; An-Ge Zhang 0000-0003-4772-1254; Tian-Qi Zhao 0000-0002-1938-1419; Chong-Yan Chen 0000-0003-2749-4891.

S-Editor: Fan JR
L-Editor: Kerr C Wang TQ
P-Editor: Fan JR

REFERENCES

1 **Sung H**, Ferlay J, Siegel RL, Laversanne M, Soerjomataram I, Jemal A, Bray F. Global Cancer Statistics 2020: GLOBOCAN Estimates of Incidence and Mortality Worldwide for 36 Cancers in 185 Countries. *CA Cancer J Clin* 2021; **71**: 209-249 [PMID: 33538338 DOI: 10.3322/caac.21660]
2 **Banks M**, Graham D, Jansen M, Gotoda T, Coda S, di Pietro M, Uedo N, Bhandari P, Pritchard DM, Kuipers EJ, Rodriguez-Justo M, Novelli MR, Ragunath K, Shepherd N, Dinis-Ribeiro M. British Society of Gastroenterology guidelines on the diagnosis and management of patients at risk of gastric adenocarcinoma. *Gut* 2019; **68**: 1545-1575 [PMID: 31278206 DOI: 10.1136/gutjnl-2018-318126]
3 **Farge D**, Bounameaux H, Brenner B, Cajfinger F, Debourdeau P, Khorana AA, Pabinger I, Solymoss S, Douketis J, Kakkar A. International clinical practice guidelines including guidance for direct oral anticoagulants in the treatment and prophylaxis of venous thromboembolism in patients with cancer. *Lancet Oncol* 2016; **17**: e452-e466 [PMID: 27733271 DOI: 10.1016/S1470-2045(16)30369-2]
4 **Kang MJ**, Ryoo BY, Ryu MH, Koo DH, Chang HM, Lee JL, Kim TW, Kang YK. Venous thromboembolism (VTE) in patients with advanced gastric cancer: an Asian experience. *Eur J Cancer* 2012; **48**: 492-500 [PMID: 22169121 DOI: 10.1016/j.ejca.2011.11.016]
5 **Khan F**, Tritschler T, Kahn SR, Rodger MA. Venous thromboembolism. *Lancet* 2021; **398**: 64-77 [PMID: 33984268 DOI: 10.1016/S0140-6736(20)32658-1]
6 **Tanizawa Y**, Bando E, Kawamura T, Tokunaga M, Makuuchi R, Iida K, Nanri K, Yoneyama M, Terashima M. Prevalence of deep venous thrombosis detected by ultrasonography before surgery in patients with gastric cancer: a retrospective study of 1140 consecutive patients. *Gastric Cancer* 2017; **20**: 878-886 [PMID: 27987041 DOI: 10.1007/s10120-016-0677-2]
7 **Jung YJ**, Seo HS, Park CH, Jeon HM, Kim JI, Yim HW, Song KY. Venous Thromboembolism Incidence and Prophylaxis Use After Gastrectomy Among Korean Patients With Gastric Adenocarcinoma: The PROTECTOR Randomized Clinical Trial. *JAMA Surg* 2018; **153**: 939-946 [PMID: 30027281 DOI: 10.1001/jamasurg.2018.2081]
8 **Wada T**, Fujiwara H, Morita S, Fukagawa T, Katai H. Incidence of and risk factors for preoperative deep venous thrombosis in patients undergoing gastric cancer surgery. *Gastric Cancer* 2017; **20**: 872-877 [PMID: 28120128 DOI: 10.1007/s10120-017-0690-0]
9 **Osaki T**, Saito H, Fukumoto Y, Kono Y, Murakami Y, Shishido Y, Kuroda H, Matsunaga T, Sato K, Hirooka Y, Fujiwara Y. Risk and incidence of perioperative deep vein thrombosis in patients undergoing gastric cancer surgery. *Surg Today* 2018; **48**: 525-533 [PMID: 29234961 DOI: 10.1007/s00595-017-1617-4]
10 **Varki A**. Trousseau's syndrome: multiple definitions and multiple mechanisms. *Blood* 2007; **110**: 1723-1729 [PMID: 17496204 DOI: 10.1182/blood-2006-10-053736]
11 **Brinkmann V**, Reichard U, Goosmann C, Fauler B, Uhlemann Y, Weiss DS, Weinrauch Y, Zychlinsky A. Neutrophil extracellular traps kill bacteria. *Science* 2004; **303**: 1532-1535 [PMID: 15001782 DOI: 10.1126/science.1092385]
12 **Brinkmann V**, Zychlinsky A. Beneficial suicide: why neutrophils die to make NETs. *Nat Rev Microbiol* 2007; **5**: 577-582 [PMID: 17632569 DOI: 10.1038/nrmicro1710]
13 **McDonald B**, Urrutia R, Yipp BG, Jenne CN, Kubes P. Intravascular neutrophil extracellular traps capture bacteria from the bloodstream during sepsis. *Cell Host Microbe* 2012; **12**: 324-333 [PMID: 22980329 DOI: 10.1016/j.chom.2012.06.011]
14 **Zeng H**, Fu X, Cai J, Sun C, Yu M, Peng Y, Zhuang J, Chen J, Chen H, Yu Q, Xu C, Zhou H, Cao Y, Hu L, Li J, Cao S, Gu C, Yan F, Chen G. Neutrophil Extracellular Traps may be a Potential Target for Treating Early Brain Injury in Subarachnoid Hemorrhage. *Transl Stroke Res* 2022; **13**: 112-131 [PMID: 33852132 DOI: 10.1007/s12975-021-00909-1]
15 **Zuo Y**, Yalavarthi S, Gockman K, Madison JA, Gudjonsson JE, Kahlenberg JM, Joseph McCune W, Bockenstedt PL, Karp DR, Knight JS. Anti-Neutrophil Extracellular Trap Antibodies and Impaired Neutrophil Extracellular Trap Degradation in Antiphospholipid Syndrome. *Arthritis Rheumatol* 2020; **72**: 2130-2135 [PMID: 32729667 DOI: 10.1002/art.41460]
16 **Cichon I**, Ortmann W, Bednarz A, Lenartowicz M, Kolaczkowska E. Reduced Neutrophil Extracellular Trap (NET) Formation During Systemic Inflammation in Mice With Menkes Disease and Wilson Disease: Copper Requirement for NET Release. *Front Immunol* 2019; **10**: 3021 [PMID: 32010131 DOI: 10.3389/fimmu.2019.03021]
17 **Marcos V**, Zhou Z, Yildirim AO, Bohla A, Hector A, Vitkov L, Wiedenbauer EM, Krautgartner WD, Stoiber W, Belohradsky BH, Rieber N, Kormann M, Koller B, Roscher A, Roos D, Griese M, Eickelberg O, Döring G, Mall MA, Hartl D. CXCR2 mediates NADPH oxidase-independent neutrophil extracellular trap formation in cystic fibrosis airway inflammation. *Nat Med* 2010; **16**: 1018-1023 [PMID: 20818377 DOI: 10.1038/nm.2209]
18 **Martins-Cardoso K**, Almeida VH, Bagri KM, Rossi MID, Mermelstein CS, König S, Monteiro RQ. Neutrophil Extracellular Traps (NETs) Promote Pro-Metastatic Phenotype in Human Breast Cancer Cells through Epithelial-Mesenchymal Transition. *Cancers (Basel)* 2020; **12** [PMID: 32545405 DOI: 10.3390/cancers12061542]
19 **Demers M**, Krause DS, Schatzberg D, Martinod K, Voorhees JR, Fuchs TA, Scadden DT, Wagner DD. Cancers predispose neutrophils to release extracellular DNA traps that contribute to cancer-associated thrombosis. *Proc Natl Acad Sci U S A* 2012; **109**: 13076-13081 [PMID: 22826226 DOI: 10.1073/pnas.1200419109]
20 **Thålin C**, Hisada Y, Lundström S, Mackman N, Wallén H. Neutrophil Extracellular Traps: Villains and Targets in Arterial, Venous, and Cancer-Associated Thrombosis. *Arterioscler Thromb Vasc Biol* 2019; **39**: 1724-1738 [PMID: 31315434 DOI: 10.1161/ATVBAHA.119.312463]
21 **Gomes T**, Várady CBS, Lourenço AL, Mizurini DM, Rondon AMR, Leal AC, Gonçalves BS, Bou-Habib DC, Medei E, Monteiro RQ. IL-1β Blockade Attenuates Thrombosis in a Neutrophil Extracellular Trap-Dependent Breast Cancer Model.

Front Immunol 2019; **10**: 2088 [PMID: 31552036 DOI: 10.3389/fimmu.2019.02088]
22 **Abdol Razak N**, Elaskalani O, Metharom P. Pancreatic Cancer-Induced Neutrophil Extracellular Traps: A Potential Contributor to Cancer-Associated Thrombosis. *Int J Mol Sci* 2017; **18** [PMID: 28245569 DOI: 10.3390/ijms18030487]
23 **Yang C**, Sun W, Cui W, Li X, Yao J, Jia X, Li C, Wu H, Hu Z, Zou X. Procoagulant role of neutrophil extracellular traps in patients with gastric cancer. *Int J Clin Exp Pathol* 2015; **8**: 14075-14086 [PMID: 26823721]
24 **Zhao L**, Bi Y, Kou J, Shi J, Piao D. Phosphatidylserine exposing-platelets and microparticles promote procoagulant activity in colon cancer patients. *J Exp Clin Cancer Res* 2016; **35**: 54 [PMID: 27015840 DOI: 10.1186/s13046-016-0328-9]
25 **Suzuki-Inoue K**. Platelets and cancer-associated thrombosis: focusing on the platelet activation receptor CLEC-2 and podoplanin. *Blood* 2019; **134**: 1912-1918 [PMID: 31778548 DOI: 10.1182/blood.2019001388]
26 **Gasiorowska A**, Talar-Wojnarowska R, Kaczka A, Borkowska A, Czupryniak L, Małecka-Panas E. Subclinical Inflammation and Endothelial Dysfunction in Patients with Chronic Pancreatitis and Newly Diagnosed Pancreatic Cancer. *Dig Dis Sci* 2016; **61**: 1121-1129 [PMID: 26597191 DOI: 10.1007/s10620-015-3972-6]
27 **Chang Z**, Zhang Y, Liu J, Zheng Y, Li H, Kong Y, Li P, Peng H, Shi Y, Cao B, Ran F, Chen Y, Song Y, Ye Q, Ding L. Snail promotes the generation of vascular endothelium by breast cancer cells. *Cell Death Dis* 2020; **11**: 457 [PMID: 32541667 DOI: 10.1038/s41419-020-2651-5]
28 **Li B**, Liu Y, Hu T, Zhang Y, Zhang C, Li T, Wang C, Dong Z, Novakovic VA, Shi J. Neutrophil extracellular traps enhance procoagulant activity in patients with oral squamous cell carcinoma. *J Cancer Res Clin Oncol* 2019; **145**: 1695-1707 [PMID: 31020419 DOI: 10.1007/s00432-019-02922-2]
29 **Zhang J**, Yu M, Liu B, Zhou P, Zuo N, Wang Y, Feng Y, Zhang Y, Wang J, He Y, Wu Y, Dong Z, Hong L, Shi J. Neutrophil extracellular traps enhance procoagulant activity and thrombotic tendency in patients with obstructive jaundice. *Liver Int* 2021; **41**: 333-347 [PMID: 33159371 DOI: 10.1111/liv.14725]
30 **Li T**, Wang C, Liu Y, Li B, Zhang W, Wang L, Yu M, Zhao X, Du J, Zhang J, Dong Z, Jiang T, Xie R, Ma R, Fang S, Zhou J, Shi J. Neutrophil Extracellular Traps Induce Intestinal Damage and Thrombotic Tendency in Inflammatory Bowel Disease. *J Crohns Colitis* 2020; **14**: 240-253 [PMID: 31325355 DOI: 10.1093/ecco-jcc/jjz132]
31 **Edge SB**, Compton CC. The American Joint Committee on Cancer: the 7th edition of the AJCC cancer staging manual and the future of TNM. *Ann Surg Oncol* 2010; **17**: 1471-1474 [PMID: 20180029 DOI: 10.1245/s10434-010-0985-4]
32 **Koupenova M**, Corkrey HA, Vitseva O, Manni G, Pang CJ, Clancy L, Yao C, Rade J, Levy D, Wang JP, Finberg RW, Kurt-Jones EA, Freedman JE. The role of platelets in mediating a response to human influenza infection. *Nat Commun* 2019; **10**: 1780 [PMID: 30992428 DOI: 10.1038/s41467-019-09607-x]
33 **Brill A**, Fuchs TA, Chauhan AK, Yang JJ, De Meyer SF, Köllnberger M, Wakefield TW, Lämmle B, Massberg S, Wagner DD. von Willebrand factor-mediated platelet adhesion is critical for deep vein thrombosis in mouse models. *Blood* 2011; **117**: 1400-1407 [PMID: 20959603 DOI: 10.1182/blood-2010-05-287623]
34 **Yang LY**, Luo Q, Lu L, Zhu WW, Sun HT, Wei R, Lin ZF, Wang XY, Wang CQ, Lu M, Jia HL, Chen JH, Zhang JB, Qin LX. Increased neutrophil extracellular traps promote metastasis potential of hepatocellular carcinoma *via* provoking tumorous inflammatory response. *J Hematol Oncol* 2020; **13**: 3 [PMID: 31907001 DOI: 10.1186/s13045-019-0836-0]
35 **Folco EJ**, Mawson TL, Vromman A, Bernardes-Souza B, Franck G, Persson O, Nakamura M, Newton G, Luscinskas FW, Libby P. Neutrophil Extracellular Traps Induce Endothelial Cell Activation and Tissue Factor Production Through Interleukin-1α and Cathepsin G. *Arterioscler Thromb Vasc Biol* 2018; **38**: 1901-1912 [PMID: 29976772 DOI: 10.1161/ATVBAHA.118.311150]
36 **Zhou P**, Li T, Jin J, Liu Y, Li B, Sun Q, Tian J, Zhao H, Liu Z, Ma S, Zhang S, Novakovic VA, Shi J, Hu S. Interactions between neutrophil extracellular traps and activated platelets enhance procoagulant activity in acute stroke patients with ICA occlusion. *EBioMedicine* 2020; **53**: 102671 [PMID: 32114386 DOI: 10.1016/j.ebiom.2020.102671]
37 **Brill A**, Fuchs TA, Savchenko AS, Thomas GM, Martinod K, De Meyer SF, Bhandari AA, Wagner DD. Neutrophil extracellular traps promote deep vein thrombosis in mice. *J Thromb Haemost* 2012; **10**: 136-144 [PMID: 22044575 DOI: 10.1111/j.1538-7836.2011.04544.x]
38 **Najmeh S**, Cools-Lartigue J, Giannias B, Spicer J, Ferri LE. Simplified Human Neutrophil Extracellular Traps (NETs) Isolation and Handling. *J Vis Exp* 2015 [PMID: 25938591 DOI: 10.3791/52687]
39 **Fuchs TA**, Brill A, Duerschmied D, Schatzberg D, Monestier M, Myers DD Jr, Wrobleski SK, Wakefield TW, Hartwig JH, Wagner DD. Extracellular DNA traps promote thrombosis. *Proc Natl Acad Sci U S A* 2010; **107**: 15880-15885 [PMID: 20798043 DOI: 10.1073/pnas.1005743107]
40 **Bodac A**, Meylan E. Neutrophil metabolism in the cancer context. *Semin Immunol* 2021; 101583 [PMID: 34963565 DOI: 10.1016/j.smim.2021.101583]
41 **Ustyanovska Avtenyuk N**, Visser N, Bremer E, Wiersma VR. The Neutrophil: The Underdog That Packs a Punch in the Fight against Cancer. *Int J Mol Sci* 2020; **21** [PMID: 33105656 DOI: 10.3390/ijms21217820]
42 **Zha C**, Meng X, Li L, Mi S, Qian D, Li Z, Wu P, Hu S, Zhao S, Cai J, Liu Y. Neutrophil extracellular traps mediate the crosstalk between glioma progression and the tumor microenvironment **via** the HMGB1/RAGE/IL-8 axis. *Cancer Biol Med* 2020; **17**: 154-168 [PMID: 32296583 DOI: 10.20892/j.issn.2095-3941.2019.0353]
43 **Itatani Y**, Yamamoto T, Zhong C, Molinolo AA, Ruppel J, Hegde P, Taketo MM, Ferrara N. Suppressing neutrophil-dependent angiogenesis abrogates resistance to anti-VEGF antibody in a genetic model of colorectal cancer. *Proc Natl Acad Sci U S A* 2020; **117**: 21598-21608 [PMID: 32817421 DOI: 10.1073/pnas.2008112117]
44 **Tohme S**, Yazdani HO, Al-Khafaji AB, Chidi AP, Loughran P, Mowen K, Wang Y, Simmons RL, Huang H, Tsung A. Neutrophil Extracellular Traps Promote the Development and Progression of Liver Metastases after Surgical Stress. *Cancer Res* 2016; **76**: 1367-1380 [PMID: 26759232 DOI: 10.1158/0008-5472.CAN-15-1591]
45 **Wolach O**, Sellar RS, Martinod K, Cherpokova D, McConkey M, Chappell RJ, Silver AJ, Adams D, Castellano CA, Schneider RK, Padera RF, DeAngelo DJ, Wadleigh M, Steensma DP, Galinsky I, Stone RM, Genovese G, McCarroll SA, Iliadou B, Hultman C, Neuberg D, Mullally A, Wagner DD, Ebert BL. Increased neutrophil extracellular trap formation promotes thrombosis in myeloproliferative neoplasms. *Sci Transl Med* 2018; **10** [PMID: 29643232 DOI: 10.1126/scitranslmed.aan8292]
46 **Zhu T**, Zou X, Yang C, Li L, Wang B, Li R, Li H, Xu Z, Huang D, Wu Q. Neutrophil extracellular traps promote gastric

cancer metastasis by inducing epithelialmesenchymal transition. *Int J Mol Med* 2021; **48** [PMID: 34013374 DOI: 10.3892/ijmm.2021.4960]

47 **Li R**, Zou X, Zhu T, Xu H, Li X, Zhu L. Destruction of Neutrophil Extracellular Traps Promotes the Apoptosis and Inhibits the Invasion of Gastric Cancer Cells by Regulating the Expression of Bcl-2, Bax and NF-κB. *Onco Targets Ther* 2020; **13**: 5271-5281 [PMID: 32606746 DOI: 10.2147/OTT.S227331]

48 **Zhang Y**, Hu Y, Ma C, Sun H, Wei X, Li M, Wei W, Zhang F, Yang F, Wang H, Gu K. Diagnostic, Therapeutic Predictive, and Prognostic Value of Neutrophil Extracellular Traps in Patients With Gastric Adenocarcinoma. *Front Oncol* 2020; **10**: 1036 [PMID: 32714865 DOI: 10.3389/fonc.2020.01036]

49 **Keshari RS**, Jyoti A, Dubey M, Kothari N, Kohli M, Bogra J, Barthwal MK, Dikshit M. Cytokines induced neutrophil extracellular traps formation: implication for the inflammatory disease condition. *PLoS One* 2012; **7**: e48111 [PMID: 23110185 DOI: 10.1371/journal.pone.0048111]

50 **Liu Y**, Yan W, Tohme S, Chen M, Fu Y, Tian D, Lotze M, Tang D, Tsung A. Hypoxia induced HMGB1 and mitochondrial DNA interactions mediate tumor growth in hepatocellular carcinoma through Toll-like receptor 9. *J Hepatol* 2015; **63**: 114-121 [PMID: 25681553 DOI: 10.1016/j.jhep.2015.02.009]

51 **Harper MT**, Poole AW. Chloride channels are necessary for full platelet phosphatidylserine exposure and procoagulant activity. *Cell Death Dis* 2013; **4**: e969 [PMID: 24357800 DOI: 10.1038/cddis.2013.495]

52 **Cleary SJ**, Hobbs C, Amison RT, Arnold S, O'Shaughnessy BG, Lefrançais E, Mallavia B, Looney MR, Page CP, Pitchford SC. LPS-induced Lung Platelet Recruitment Occurs Independently from Neutrophils, PSGL-1, and P-Selectin. *Am J Respir Cell Mol Biol* 2019; **61**: 232-243 [PMID: 30768917 DOI: 10.1165/rcmb.2018-0182OC]

53 **Zhang Y**, Wang C, Yu M, Zhao X, Du J, Li Y, Jing H, Dong Z, Kou J, Bi Y, Novakovic VA, Zhou J, Shi J. Neutrophil extracellular traps induced by activated platelets contribute to procoagulant activity in patients with colorectal cancer. *Thromb Res* 2019; **180**: 87-97 [PMID: 31271975 DOI: 10.1016/j.thromres.2019.06.005]

54 **Martinod K**, Witsch T, Farley K, Gallant M, Remold-O'Donnell E, Wagner DD. Neutrophil elastase-deficient mice form neutrophil extracellular traps in an experimental model of deep vein thrombosis. *J Thromb Haemost* 2016; **14**: 551-558 [PMID: 26712312 DOI: 10.1111/jth.13239]

Published by **Baishideng Publishing Group Inc**
7041 Koll Center Parkway, Suite 160, Pleasanton, CA 94566, USA
Telephone: +1-925-3991568
E-mail: bpgoffice@wjgnet.com
Help Desk: https://www.f6publishing.com/helpdesk
https://www.wjgnet.com